APPLICATION OF A CHEMICAL HEAT PUMP ON HIGH-TEMPERATURE HEAT PROCESS FOR HIGH EFFICIENCY ENERGY UTILIZATION

Yukitaka Kato, Mitsuteru Yamada, Yoshio Yoshizawa,
Research Laboratory for Nuclear Reactors,
Tokyo Institute of Technology, Tokyo , Japan

Abstract

The thermal performance of a chemical heat pump that used a reaction system of calcium oxide/lead oxide/carbon dioxide, which was developed for utilization of high-temperature heat above 800^{o}C, was studied experimentally. The thermal performance of a packed bed reactor of a calcium oxide/carbon dioxide reaction system, which stored and transformed a high-temperature heat source in the heat pump operation, was examined under various heat pump operation conditions. The energy analysis based on the experiment showed that it was possible to utilize high-temperature heat with this heat pump. This heat pump can store heat above 850^{o}C and then transform it into a heat above 900^{o}C under a pressure near atmosphere. The validity of the heat pump was estimated by a numerical thermal analysis of the experimental reactor.

KEYWORDS

Chemical Heat Pump, Calcium Oxide, Lead Oxide, Carbon Dioxide, Packed Bed Reactor

INTRODUCTION

High-temperature processes such as those involved in iron smelting, fuel cells, solar energy collectors and high temperature gas reactors, produce a large amount of high-temperature heat above 800 ^{o}C. This heat may be used as the heat source for various heat utilization systems due to its high quality. On the other hand, the disagreement between the high-temperature heat production amount and heat consumption one is anticipated in a practical use. In order to realize efficient and stable utilization of the high-temperature heat, heat storage and transformation technologies need to be devised. A chemical heat pump is one candidate for such improvements, because this device can be applied for a wide temperature range with little heat loss for long periods of time. A calcium oxide/carbon dioxide (CaO/CO_2) reaction system appears to be suitable for a high-temperature heat pump above 700^{o}C [1, 2].

The key consideration in the development of such a heat pump system that uses this reaction is how to handle and store the carbon dioxide gas phase reactant. In our previous study, a lead oxide/carbon dioxide (PbO/CO_2) reaction system is demonstrated to be effective for storing carbon dioxide [3]. Based on this finding, a heat pump that combines both PbO/CO_2 and CaO/CO_2 reactions to form a calcium oxide/lead oxide/carbon dioxide ($CaO/PbO/CO_2$) system is proposed [4]. Heat pump effectiveness at temperatures above 830 ^{o}C under atmospheric pressure was reported in a kinetic study on a thermobalance, in which the possibility of thermal drivability of the heat pump was also demonstrated. Thermal drivability is preferable for a practical heat pump because no mechanical work is required, thus enabling simple, safe and low-cost development. Based on the above-mentioned thermal analysis, the present study examines a packed bed reactor of a CaO/CO_2 reaction system, primarily in order to evaluate the heat pump thermal output performance. Because a packed bed reactor is employed for a common practical reactor and the reactor is a complex system involving chemical reaction, mass transfer and heat conduction, a bed reactor experiment is required in order to design a practical reactor. Then, heat storage and heat output operations of the CaO/CO_2 bed reactor were examined under various reaction conditions in the present study. Based on the results of the packed bed experiment, the thermal performance of the heat pump was evaluated numerically.

Principle of the Heat Pump

The following CaO/CO_2 and PbO/CO_2 reaction systems are used in the $CaO/PbO/CO_2$ chemical heat pump:

$$CaO(s)+CO_2(g)=CaCO_3(s),\ \Delta H°_1=-178.3\text{kJ/mol} \quad (1)$$

$$PbO(s)+CO_2(g)=PbCO_3(s),\ \Delta H°_2=-88.3\text{kJ/mol} \quad (2)$$

The basic system of a heat transformer type of the heat pump is shown in Fig. 1. The equilibrium relationship of the heat pump operation is depicted in Fig. 2. Each enclosed number in Fig. 2 corresponds to the same number in Fig. 1. Figure 2 shows one example of a heat pump operation process based on the previous thermobalance study [5]. Heat at a higher temperature than the original heat source can be obtained by this operation. The heat pump system consists of a CaO reactor and a PbO reactor. Operation of the heat pump involves (a) a heat storage mode and (b) a heat supply mode, as indicated in Fig. 1. Initially, $CaCO_3$ and PbO are charged into each reactor. In the storage mode, the CaO reactor bed receives heat from a heat source at temperature T_d. Subsequently, CaO and CO_2 are formed as a result of the decarbonation of $CaCO_3$. CO_2 reacts with PbO in the PbO reactor at pressure P_{2c} and the exothermic heat of the carbonation is recovered at temperature T_{2c}, yielding $PbCO_3$. In the heat supply mode, the decarbonation of $PbCO_3$ proceeds in the PbO reactor using heat at temperature T_{2d} (which is higher than T_{2c}). CO_2 formed at pressure P_{2d} (which is higher than P_{2c}) is introduced into the CaO reactor. The carbonation of CaO then proceeds and heat is generated exothermically in the reactor at temperature T_c (which is higher than T_d) due to the higher reaction pressure. Since this process drives thermally, using chemical reactions, the coefficient of performance, COP, which is defined as the ratio of the carbonation heat output to the decarbonation stored heat, is expected to be close to unity.

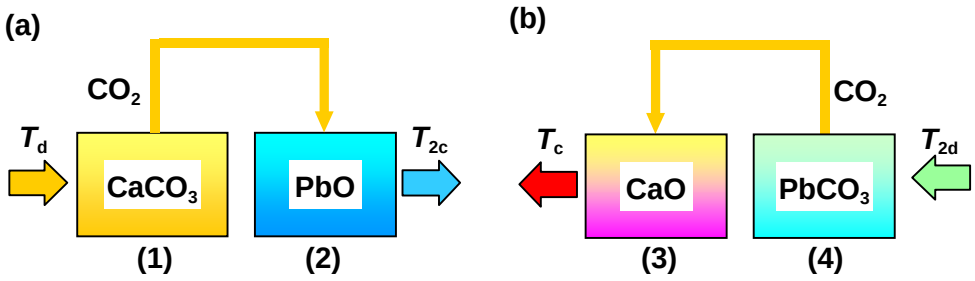

Fig. 1 Principle of the $CaO/PbO/CO_2$ chemical heat pump

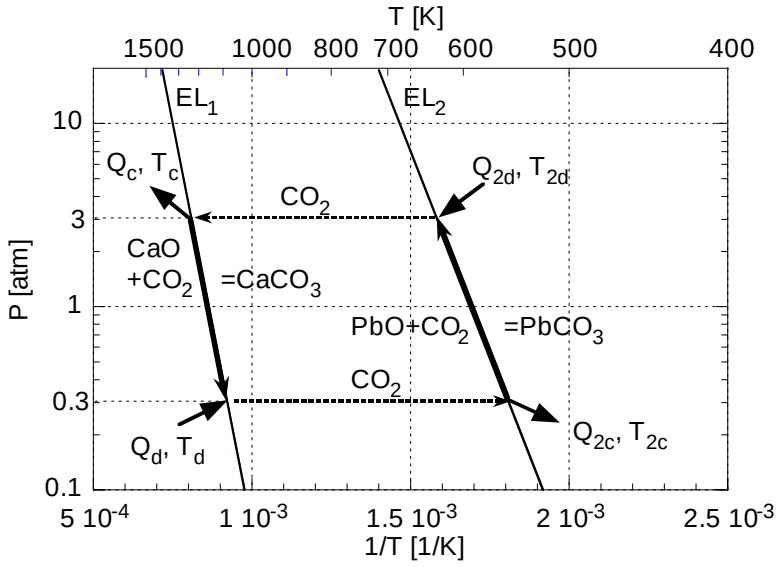

Fig. 2 Equilibrium relationship of the heat pump.

EXPERIMENT

The kinetics of the CaO/CO_2 reaction were studied using a packed bed reactor under various reaction conditions in order to evaluate the thermal performance of the heat pump.

Figure 3 shows an experimental apparatus system for reactivity measurement of a CaO/CO_2 packed bed reactor. The system is composed of a reactor vessel, gas supply and measurement systems. The alumina reactor tube having 60 mm of inner diameter is positioned vertically inside the vessel and surrounded with insulation. A joule heating wire is coiled around the outside of the reactor tube. A steel mesh tube having a diameter of 20 mm is positioned centrally inside the reactor tube as a carbon dioxide gas pass. Particle reactant (1.0 kg) of $CaCO_3$ was packed inside the reactor tube to a height of 300 mm. Natural calcium carbonate (produced from Hiroshima, Japan, 98% purity, particle diameter 1.0 - 2.0 mm) was used in the experiment. Thermocouples were installed in some parts of the reactant bed for measuring the bed temperature change. The temperature at the outside surface of the bed (i.e. the inside wall of the reactor tube) at a position 135 mm in height from the bottom of the bed was considered to be the reference bed temperature and was maintained using an electric heater. The weight change of the reactor vessel during reaction was monitored continuously by a balance and the reacted fraction was calculated based on the change in weight.

The experiment was started from the decarbonation of $CaCO_3$. Decarbonation proceeded at a temperature that was controlled by the heater under a constant pressure. The carbonation followed the decarbonation and was measured after the bed temperature had become steady at a carbonation temperature that was controlled by heating. The heating was cut off at the start of the carbonation, and then carbon dioxide was introduced to the reactor while the pressure was maintained by the pressure regulator system. A mole reacted fraction, x [%], is defined as follows:

$$x = \left\{1 + \frac{\Delta m / M_{CO2}}{m_{ini} / M_{CaCO3}}\right\} \times 100 \qquad (3)$$

x=0 % and 100 % depict 100 mol% of CaO and $CaCO_3$, respectively.

EXPERIMENTAL RESULTS

Decarbonation of $CaCO_3$

The dependency of the decarbonation reactivity on the reaction pressure (P_d) at 850 and 900 °C of the reference bed temperature (T_d) is shown in Fig. 4. Higher reactivity was measured under lower pressure and higher temperature. The reaction saturated at approximately 10–30 %. The previous thermobalance experiment shows that the decarbonation proceeds almost completely under these

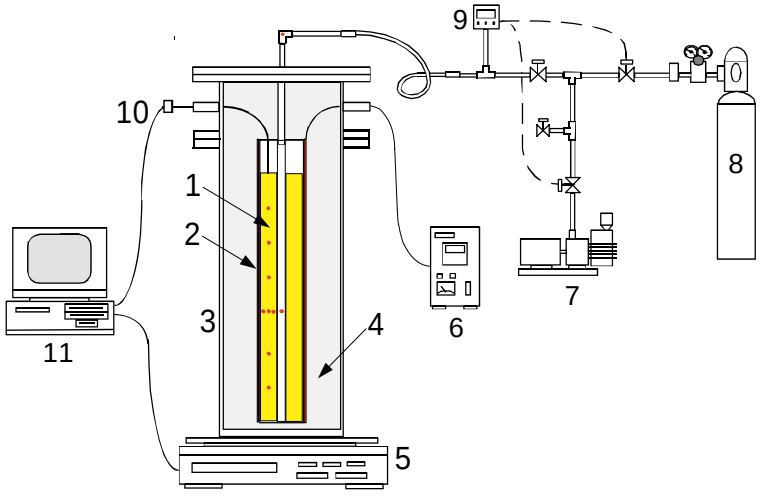

Fig. 3 Experimental apparatus; (1) reactor bed, (2) reactor tube, (3) reactor vessel, (4) insulation, (5) balance, (6) heating controller, (7) vacuum pump, (8) CO_2 bomb, (9) pressure regulation system, (10) Thermocouples, (11) personal computer

conditions [5]. Because the temperature distribution in the reactor bed was not homogeneous and regions at temperatures lower than T_d existed in some parts of the bed, the reaction did not complete in some parts of the bed and x did not reach 0 %.

Carbonation of CaO

An example of the carbonation operation results is shown in Fig. 5. Reaction bed temperature (T_{bed}) distribution and reacted fraction changes are shown in the figure. The reference temperature was maintained at the initial temperature ($T_{c,ini}$) of 900°C before the reaction. After cutting off of joule heating and introducing carbon dioxide at t_c=0 min, the reaction proceeded and the reactor bed temperature almost attained the reaction equilibrium temperature of 895°C. Length values in the temperature's legend show the measured position height from the bottom of the bed. The reaction process was then controlled by the heat conduction in the bed. After the heat generation of carbonation became smaller than the heat conduction loss, the reactor bed temperature started to decrease, and subsequently the change of the reacted fraction slowed. The temperature at a position 205 mm in height decreased faster than the temperatures at all other positions. This position was colder than the other positions because of the upward conduction loss of heat. This is shown at the initial temperature distribution at t_d= –10 – 0 min in the figure, in which the temperature was lower than those at other positions for this period. As a result, the decarbonation at this position did not proceed adequately, and the amount of the carbonation was also small. Therefore, the temperature at this position dropped faster than those at other positions. Thus, reactor design must take into account the reaction and temperature distributions. Figure 6 shows the carbonation reactivity dependency on the initial bed temperature ($T_{c,ini}$). The representative bed temperature, T_c, shows at the middle point of the radial bed thickness at a position 135 mm in height from the bottom of the bed. Each reaction attained about 70 % in approximately 100 min of t_c. Higher reactivity was obtained at lower initial temperature because lower temperature is advantageous for the exothermic carbonation from an equilibrium standpoint. Reaction at lower temperature was limited by the reaction at the beginning of the carbonation, and the initial reaction heat was converted to the sensible heat of the bed. On the other hand, carbonation operation at higher $T_{c,ini}$ attained faster to a heat conduction control than at lower $T_{c,ini}$, because the gap of the equilibrium temperature was smaller than at lower $T_{c,ini}$. Then, the exothermic reaction rate slowed easily compared with a lower temperature case. The maximum temperatures of all conditions attained about the same of the equilibrium temperature for the reaction pressure of 1.0 atm, that is, 895°C. Because all attained temperatures were close to the equilibrium temperature, the heat output temperature of the heat pump was expected to be controllable by the reaction pressure.

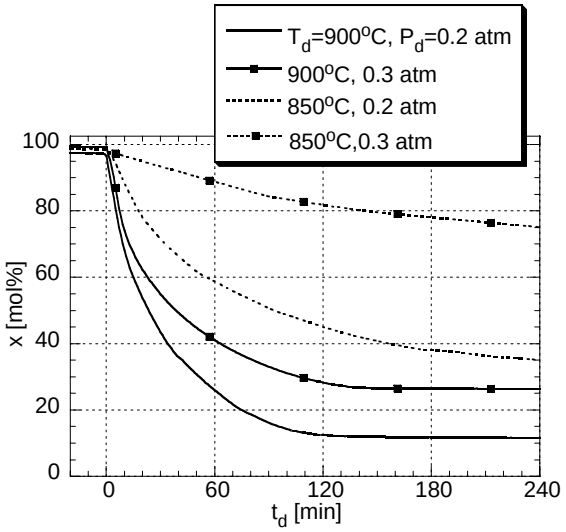

Fig. 4 Decarbonation experiment of $CaCO_3$ at T_d of 850°C and 900°C.

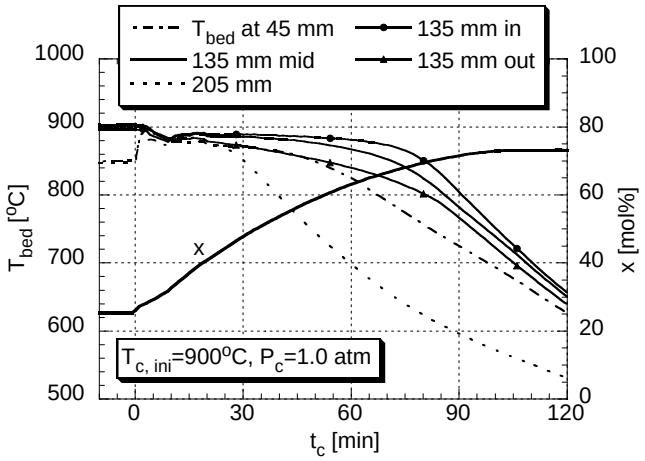

Fig. 5 Example of carbonation experiments of CaO at $T_{c,ini}$ of 900°C and P_c=1.0 atm.

DISCUSSION

The feasibility of the heat pump was evaluated numerically using the experimental results of the CaO/CO_2 reactor. The thermal performance under high-pressure carbonation was particularly discussed, because the high-pressure reaction was expected high-temperature output, which was useful to widen the heat pump applicability.

Numerical analysis

The carbonation process in the reactor bed was analyzed numerically as a transient axial symmetrical two-dimensional cylindrical heat transfer model accompanied by internal thermal energy production. A heat conduction equation of the bed is depicted as follows:

$$\rho C_v \frac{\partial T}{\partial t} = \frac{1}{r}\frac{\partial}{\partial r}\left(rk\frac{\partial T}{\partial r}\right) + \frac{\partial}{\partial z}\left(k\frac{\partial T}{\partial z}\right) + S - h \tag{4}$$

, where r shows radial length centered the symmetry axis of the bed, and z shows height from the bottom of the bed. The apparent thermal conductivity, k [W/mK], in the bed was assumed to consist of heat conduction and thermal radiation heat transfer effects by introducing a thermal conductivity, k_c [W/mK] and a radiant thermal conductivity, k_R [W/mK] as,

$$k = k_C + k_R \tag{5}$$

$$k_R = C_R T^3 \tag{6}$$

where C_R [W/mK^4] is a radiant heat transfer coefficient. The values of heat transfer parameters used for the boundary conditions and the ks were obtained from a numerical analysis based on heat conduction experiments using the reactor bed. Infinite reaction rate of the carbonation was supposed for internal energy production term (S [W/m^3]) calculation, because the heat production generated by the carbonation was relatively faster than the heat conduction in the bed at initial carbonation period as shown in Figs. 5 and 6.

Estimation Results

The calculation result under P_c=1.0 atm and $T_{c,ini}$=900^{o}C is shown in Fig. 7. The reacted fraction and bed temperature distribution changes show similar trend of the experimental result under the same condition shown in Fig. 5. However, the temperature change in the calculation was more monotonous than experimental result, because the reactor bed system in the calculation was presumed to be controlled by the heat conduction, and the temperature change depended on the heat conduction. The

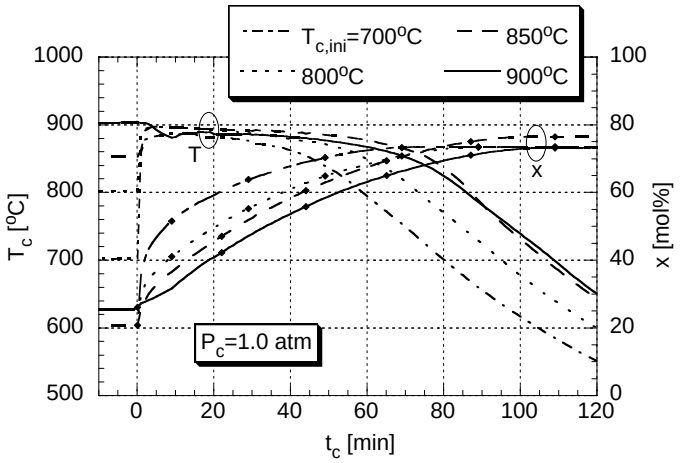

Fig. 6 Effect of initial bed temperature on CaO carbonation under P_c=1.0 atm.

relationship for the reacted fraction change between the experiment and calculation shows also similar trend. Then, the reaction rate is required to be considered for further discussion. The calculation result under a higher reaction pressure of 5.0 atm at the same $T_{c,ini}$ in Fig. 5 is shown in Fig. 8 for an estimation of the heat pump possibility. A heat output above 1000°C during about 60 min is expected in this condition. The temporal decrease in temperature is more rapidly than the case at 1.0 atm, because the temperature difference between the reactor inside and atmosphere is larger than one of the 1.0 atm case.

Because the calculation result in Fig. 7 showed almost similar trend of the experimental result in Fig. 5 around the initial period approximately until 60 min, the thermal performance of the reactor during 60 min carbonation under some reaction pressure cases were estimated. The estimation results for the attained maximum bed temperature (T_{att} [°C]), mean heat output (W_m [W/kg]), heat output amount (Q [kJ/kg]) are summarized in Table 1. The calculation and experimental results in 1.0 atm show similar values. Higher reaction pressure condition shows higher heat output power and output temperature. 237 W/kg output up to 1016°C was expected under a reaction pressure of 5.0 atm.

CONCLUSIONS

The feasibility of a CaO/PbO/CO_2 chemical heat pump was examined using experimental kinetic studies of a CaO/CO_2 reactor bed. Heat output by carbonation of CaO was confirmed experimentally at 900°C under a reaction pressure of 1.0 atm. The maximum temperature of the reactor bed attained almost the equilibrium temperature of the reaction pressure. Then, the heat output temperature of the heat pump was expected to be controllable by the reaction pressure. The thermal performance of the reactor under higher pressure condition was estimated numerically. The heat output 237 W/kg of output up to 1013°C for 60 min was expected under a pressure of 5.0 atm. The higher-pressure carbonation was expected to be available for high efficient energy utilization of heat sources.

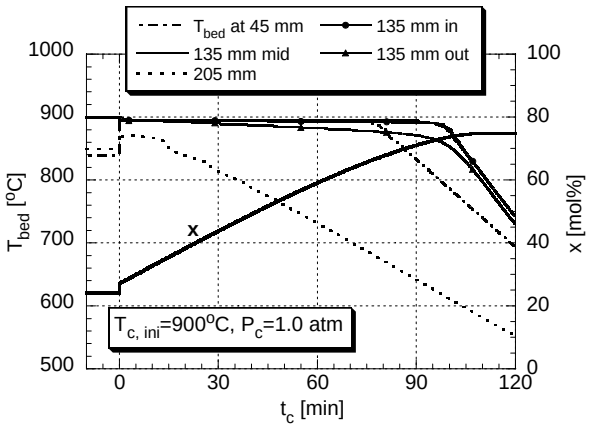

Fig. 7 Simulation result of CaO carbonation at $T_{c,ini}$ of 900°C and P_c=1.0 atm.

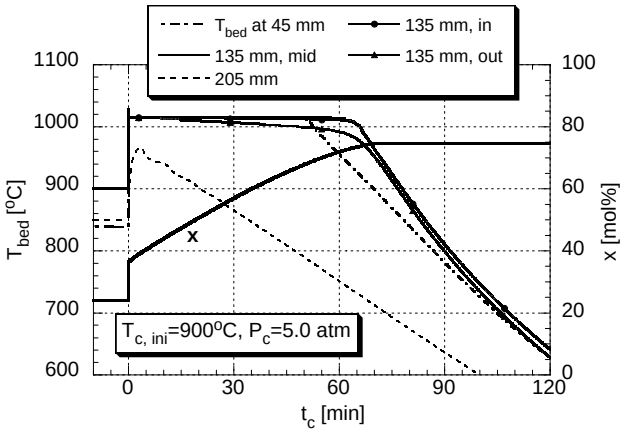

Fig. 8 Simulation result of CaO carbonation at $T_{c,ini}$ of 900°C and P_c=5.0 atm.

Table 1 Calculated thermal performance of the CaO reactor during 60 min carbonation under $T_{c,ini}$ of 900°C

	Exp.	Simulated value		
P [atm]	1.0	1.0	3.0	5.0
T_{att} [°C]	892	895	974	1016
W_m [W/kg]	180	173	218	237
Q [kJ/kg]	661	623	785	853

Nomenclature

C_R-radiant heat transfer coefficient [W/mK^4]; C_v-equivalent heat capacity of the reactor bed [J/kg.K]; h sensible heat [J/m^3];k apparent thermal conductivity of the bed [W/mK]; k_c thermal conductivity of the bed [W/mK]; k_R radiant thermal conductivity of the bed [W/mK]; m mass of reactant [kg]; P reaction pressure of CO_2 [atm]; Q heat output amount of the reactor bed by CaO carbonation [MJ/kg-$CaCO_3$]; r radial length centered the symmetry axis of the bed [m]; S internal energy production [J/m^3]; T reaction temperature [^{o}C]; $T_{c,ini}$ initial bed temperature of the CaO carbonation ;t reaction time[h]; W_m mean heat output of the reactor bed by CaO carbonation[kW/kg-$CaCO_3$]; x mole reacted fraction [mol%]; z height from the bottom of the bed [m]; Δm mass change of reactant during reactions [kg]; $\Delta H°$ standard reaction enthalpy [J/mol]; ρ density of the reactor bed [kg/m^3].

subscripts

1	CaO/CO_2 reaction system
2	PbO/CO_2 reaction system
c	carbonation
d	decarbonation
in	inside the reactor bed adjacent to the inner mesh tube
mid	middle part in the radius direction of the reactor bed
out	outside the reactor bed adjacent to the inner side of the reactor

References

1. Barker, R., “The Reactivity of Calcium Oxide Towards Carbon Dioxide and its use of Energy Storage”, *J. Appl. Chem. Biotechnol*. **24**, 1974, pp.221-227.
2. Kyaw Kyaw, Matsuda H., Hasatani M., “Applicability of Carbonation/Decarbonation Reactions to High-Temperature Thermal Energy Storage and Temperature Upgrading”, *J. Chem. Eng. Japan*. **29**, 1996, pp.119-125.
3. Kato, Y., Watanabe Y., Yoshizawa Y., “Application of Inorganic/Carbon Dioxide Reaction System to a Chemical Heat Pump”, *Proceed. 31st Intersociety Energy Conversion*, Vol. 2, 1996, pp. 763-768, Washington, D. C.
4. Kato, Y., Saku D., Harada N., Yoshizawa Y., “Utilization of High Temperature Heat Using a Calcium Oxide/Lead Oxide/Carbon Dioxide Chemical Heat Pump”, *J. Chem. Eng. Japan*. **30,** (6), 1997, pp.1013-1019.
5. Kato, Y., Harada N., Yoshizawa Y., “Kinetic Feasibility of a Chemical Heat Pump for Heat Utilization of High-Temperature Processes”, *Applied Thermal Engineering* **19**, 1999, pp.239-254.